Chemical dynamics based on methane, light backscatter, and redox potential of hydrothermal plumes at Rumble III, Kermadec arc, New Zealand

Marie Salmi
Department of Oceanography, University of Washington, Seattle, WA, 98115
maries3@u.washington.edu
http://staff.washington.edu/maries3/

Non-technical summary:

The University of Washington student scientific cruise along the Kermadec volcanic arc, north of New Zealand was performed March, 2-17, 2009. Research included characterizing the chemical and physical properties to determine the location and nature of hydrothermal plumes over Rumble III, an underwater volcano located at 35° 44.377' S, 178° 29.839' E. Rumble III is unique due to the presence of a shallow hydrothermal system that will have a mixture of chemosynthetic and photosynthetic biology present along with a high potential of interacting with the surface oceanic water. Sensors and collection bottles for water samples were attached to a rosette frame. This frame was deployed vertically over the side a stationary ship or raised and lowered in cycles through the water column while the ship was moving. My research involved comparing data from various sensors that measured particle concentration and size, oxygen and the concentrations of reduced chemical species, such as methane, reduced iron, and hydrogen sulfide that are within hydrothermal plumes and can be utilized by chemosynthetic organisms. Along with sensor measurements, methane (CH_4) concentrations were also measured from collected water samples. The hydrothermal plumes were discovered at ~250 m above the summit of the volcano that corresponded with an oxygen low, and high concentrations for particulates and reduced species. Chemosynthesis and spontaneous reactions is believed to be the reason for the anomalous low oxygen based on the relationship between the redox potential and oxygen. There was no obvious correlation between methane and redox potential. The direction of plume movement was in the north-west direction, corresponded with current velocities.

Abstract

Hydrothermal plumes over Rumble III, located at 35° 44.377' S, 178° 29.839' E within the Kermadec Arc, were characterized during a University of Washington student cruise from March 2-17, 2009. This was done using sensors that measured redox potential, particulates, and oxygen. Discreet methane (CH_4) measurements were taken near and within the plumes and analyzed onboard by a flame ionizing detecting gas chromatograph. Samples were collected with Niskin bottles attached to a CTD rosette amd deployed in a tow-yo and vertical fashion. The hydrothermal plumes were discovered ~250 m above the summit, corresponding with an oxygen low of ~175.0 μmol l^{-1}, high particulates of 1.1 ΔNTU and high concentrations of reduced species. The oxygen anomalies decreased to -28.75 μmol l^{-1} within the plume. Redox potential decreases as the particulates increases, resulting in higher concentrations of reduced species such as CH_4, Fe^{2+}, and H_2S within the plume. The redox potential was the lowest within the plume at 1.9 μmol l^{-1} while background was ~3.1 μmol l^{-1}. The increase in particulates, measured in ΔNTU, was the highest at 1.1 nephens within the main plume. The CH_4 concentrations ranged from 2.41 to 4.84 nmol l^{-1}, which had little correlation to oxygen. Oxygen concentrations decreased with redox potential and increased particulate. The lack of correlation between CH_4 and redox potential implied other mechanisms were affecting CH_4 concentration. The direction of plume movement was determined to be in the northwest direction, corresponding with current velocities.

Introduction

Hydrothermal vents are a valuable link in biogeochemical cycling because they provide a unique geochemical environment for chemosynthetic micro- and symbiont based macro- fauna, while providing a significant amounts of chemicals and heat into the oceans (Von Damm. 1995) The hydrothermal fluids are the result of chemical alteration of oceanic rocks and seawater as the fluids move through the crust at elevated temperatures after interacting with a heat source such as hot rock or magma (Von Damm. 1995). This results in metal enriched, hot and acidic plumes that carry heat and reduced chemical species from within the mantle that mixes with surrounding ocean water by hydrothermal plumes (McCollom. 2000). Research on hydrothermal vents is still highly incomplete with much of the ~20,000 km of volcanic arcs in the Pacific region still unexplored (de Ronde et al. 2001).

A reliable way of detecting hydrothermal plumes quickly and efficiently is through the use of in situ sensors, such as particulate, temperature and redox potential, along with methane (CH_4) measurements (Mottl et al. 1995). Hydrothermal vents are an important source of CH_4 to the surrounding ocean. On average, $1.3x10^8$ moles of CH_4 are estimated to be mixed into the ocean from hydrothermal vents by way of hydrothermal plumes (Kadko et al. 1995). Methane is produced in hydrothermal systems through a variety of processes including outgassing of juvenile carbon via high-temperature hydrothermal vents, thermal breakdown of complex hydrocarbons, high-temperature inorganic synthesis from CO_2 and H_2 and organic synthetic production (Welhan. 1988; Lilley et al. 1993). Typically, CH_4 from deep hydrothermal vents is on the order of 10^5 to 10^7 times higher than background seawater concentrations and can be detected up to 10's of km away from a vent site (de Angelis et al. 1993). The decreases in CH_4 concentration with increasing distance from a vent site, is caused primary by microbial

oxidation. Within 3 km from the vent site, >90 % of the CH_4 can be converted through microbial oxidation (Cowen, 2002).

The Kermadec-Tonga volcanic arc, located in the southwest Pacific, is a 2500 km subduction zone formed by the colliding and subducting of the pacific plate under the Australian plate (de Ronde et al. 2005). Within the region of north New Zealand, at 36°S, the cold and old pacific plate subducts at a rate of 50 mm yr-1 (Wright et al. 2006). Other microplates involved in this geological formation include the Niuafo'ou, Tonga, and Kermadec plates (Wright et al. 2006). The Kermadec-Tonga arc is one of the longest intra-oceanic arcs in the world and consists of at least ninety four underwater volcanoes; so far 74% of these volcanoes have been surveyed for hydrothermal activity (de Ronde et. al. 2005). The south Kermadec arc hosts 13 basaltic-andesitic stratovolcanoes with silicic caldera systems. Rumble III, located at 35° 44.377' S, 178° 29.839' E, is one of the three most hydrothermally active volcanoes of the south Kermadec arc and is a prime example of hydrothermal activity near the photic zone (Wright et. al. 2006) Rumble III is comprised of two cones and a small caldera. The small caldera has a width of 300-500 m with the southwest side is partially collapsed (Wright et al. 2002). The southern cone is the shallowest at ~ 220 m, while the central cone shoals to ~520 m. Light transmission and helium isotopes measurements made during a survey by New Zealand American PLUme mapping expedition (NZAPLUME) cruise found evidence of active venting of hydrothermal fluids at Rumble III. Although they did not find any vent sites, there was evidence of massive cone building and large lava flows (up to 8 km long) on and near the volcano (Wright et. al. 1994). Rumble III is unique because 1) the southern cone rises to within 200 m of the surface, near the photic zone and 2) because of the lower overlying hydrostatic pressure that results in lower boiling temperature linked to deposition of metals subsurface (Prol-Ledesma et al. 2005). In order to understand the effect of hydrothermal plumes over Rumble III on the surround water,

the hydrothermal plumes' distributions and locations are needed to be measured and quantified in terms of chemical abundance through the use of in situ sensors and CH_4 measurement.

Method

Shipboard analysis was done during the student cruise TN230 aboard R/V Thomas G. Thompson. Water samples were collected using 21 Niskin bottles, each 10 liter in volume, attached to a rosette. The bottles were closed at locations of interest based on real-time data from sensors attached to the rosette. These sensors included conductivity, temperature, depth and optical measurements giving the package the name 'CDTO'. The CTDO was lowered vertically and in a 'towyo' fashion in and around Rumble III. There were two tow-yos and one vertical cast with sensor and methane measured over and around Rumble III (Figure 1).

Methane samples were analyzed shipboard in a similar fashion to the method in Lilley et al. 1995 with some deviation. Water was drawn from the Niskin bottles attached to the CTDO rosette using plastic, 140 ml syringes. Each sample was checked that air bubbles were not present in the syringe as to prevent air contamination. Duplicate samples were taken from each Niskin to check for analysis error. The samples were prepared by adding a headspace of helium and shaking intensely to strip the water of methane. The water to headspace ratio was kept at 1:2 using 20 ml water and 40 ml helium. After the water equilibrated with room temperature, the headspace was injected into a flame ionizing detecting suitcase gas chromatograph (GC). GC signals were recorded and integrated using a spectra physics chromatographic integrator. Standards run on the GC included CH_4 10 ppm standards and air (atmospheric) samples taken shipboard. Standard deviation of 10 ppm standards was an average of 1.8 % of the measured values. The air concentrations had an average standard deviation that was 5.6% of the measured concentrations and ranged from 3.8-7.4 % over time for each cast. Methane concentration was

calculated by using the 10 ppm standard to the average GC output signal for 1 ppm CH4 concentration.

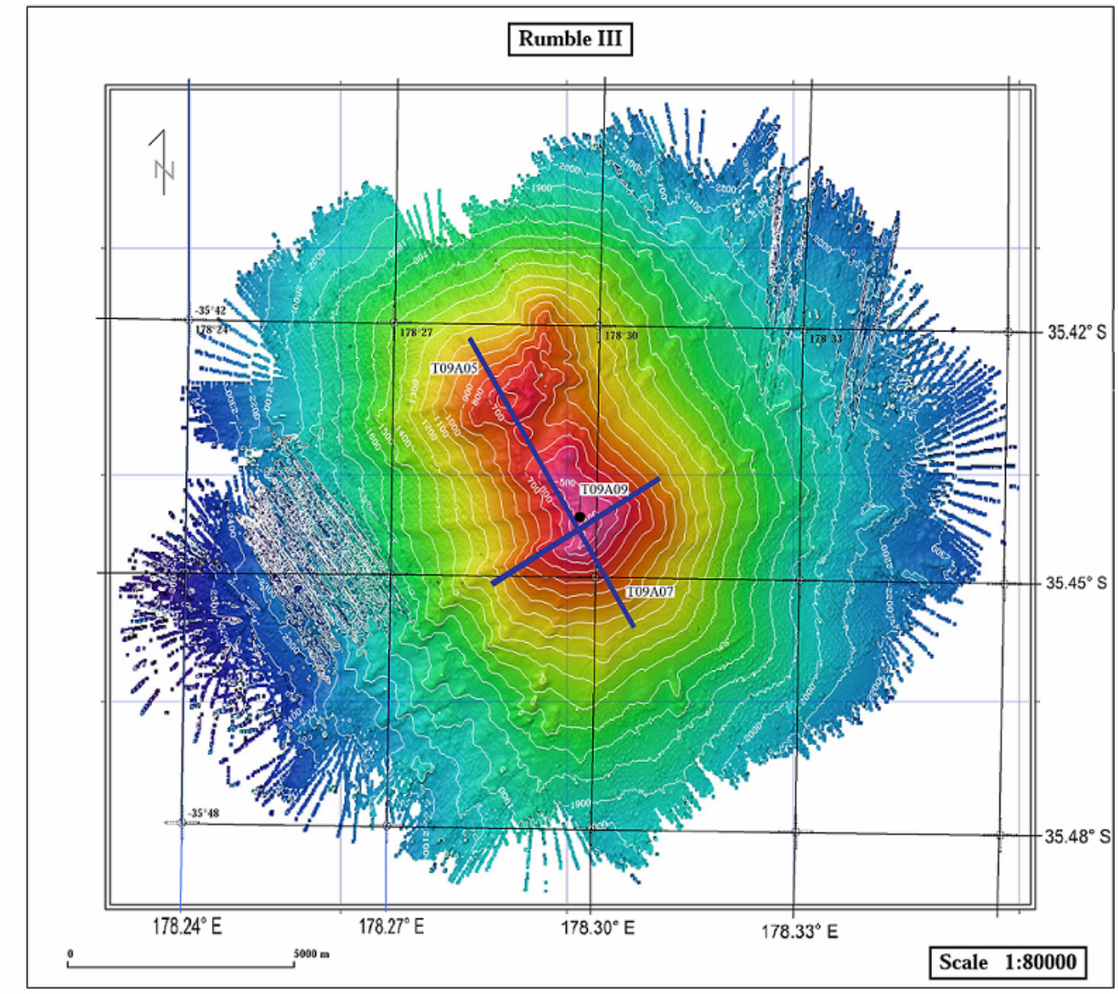

Figure 1: Location of the two tow-yos and vertical cast. T09A05 is heading from NW to SE while T09A07 was done from SW to the NE over Rumble III. The vertical cast V09A09 is marked as a black dot. (E. Dodge. pers. Com.)

The in situ sensors incorporated on the CTD included a light backscattering sensor (LBSS), redox potential, and oxygen (O2) sensors. The LBSS is a good indication of particulate sizes within hydrothermal plumes within a 95% interval (Baker et al. 2001). The redox potential was measured through the use of a platinum electrode with silver-silver chloride reference cell (S. Walker. pers. com.) that measured the amount of reduced agents present including methane, Fe^{2+}, sulfur, and H_2. The O_2 was measured in situ using a Seabird 43 oxygen sensor attached to

the CTDO. This sensor has an initial accuracy of 2% of oxygen saturation concentration, and a drift of 2% for every 1000 hours (Carlson. 2007). The particulates size and concentrations was measured using an light backscattering sensor (LBSS) in Nephelometric Turbidity Units (NTU). The particulate anomaly (ΔNTU) was calculated by finding the difference from the mid water minimum.

Results

Particulate and oxygen concentrations, and the redox potential (Figure 2; Figure 3) define the hydrothermal plume located over Rumble III. The first tow-yo, T09A05, went from NW to SE over both south and north cones. The second tow-yo, T09A07 went from SW to NE over the southern shallow cone. Both tow-yos were done during the end of ebb and into slack tidal phase, reducing any plume distribution difference based on tides. In T09A05, the lowest redox potential of ~2.2 volts (Figure 2a), indicated the highest amount of reduced agents at ~250 m depth over the summit of the volcano. From the minimum voltage, there is a gradual increase to the background of ~3.2 moving away from the summit. Measured voltage was slightly lower on the north side of the volcano in comparison to the south side, reaching the highest measured voltage at ~3.2. The difference is due to a lag in the measurement after the sensor was in contact with the high concentrations within the plume. This lag is assumed to be an artifact which is seen in both transects over the volcano. There is a sharp change in reduced species at 35.73 S near the summit, shown by a difference between the low and high voltage (Figure 2a; Figure 3a). The redox potential for tow-yoT09A07 had the lowest voltage at ~240 m near 35.732° S of 1.8 volts (Figure 3a). There is a gentle increase with depth towards north while there is a distinct change from the minimum towards the west similar to T09A05.

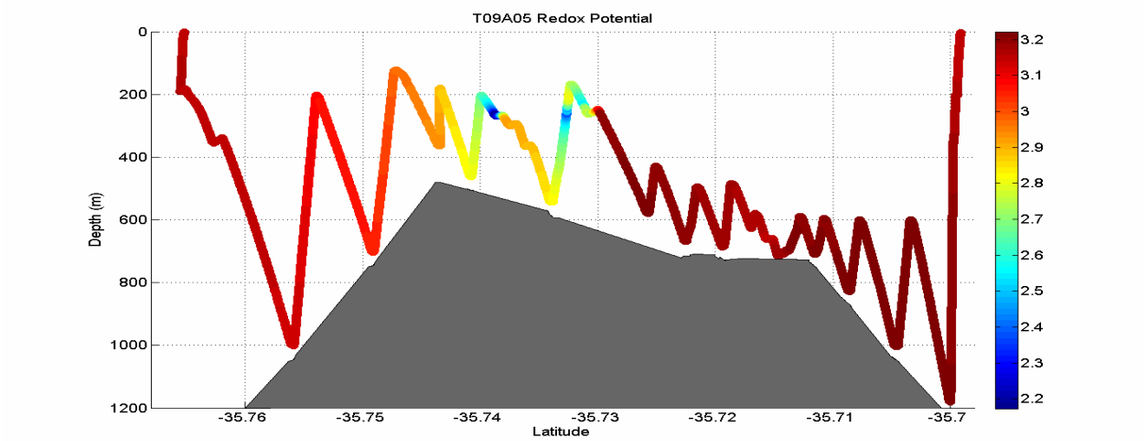

2a

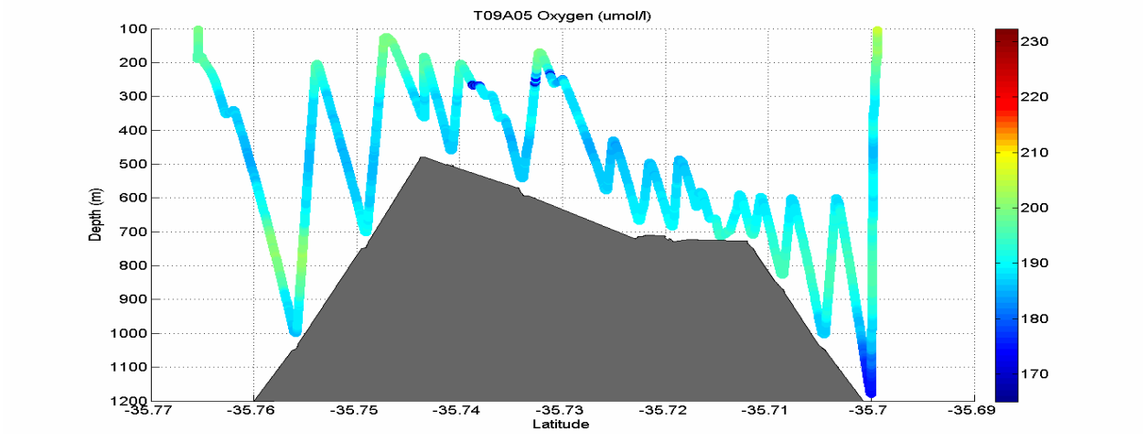

2b

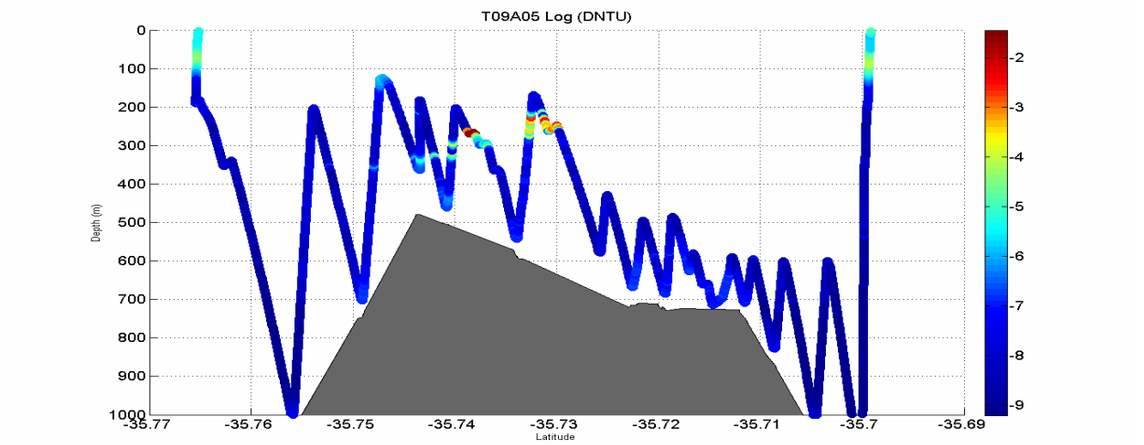

2c)

Figure 2: Tow-yo T09A05 was done from NW to SE over Rumble III and measured A) oxygen in μmol l^{-1}. B) redox potential (Volts) and C) log (ΔNTU) changes with depth along tow-yo. Topography is determined based on altimeter readings on CTDO.

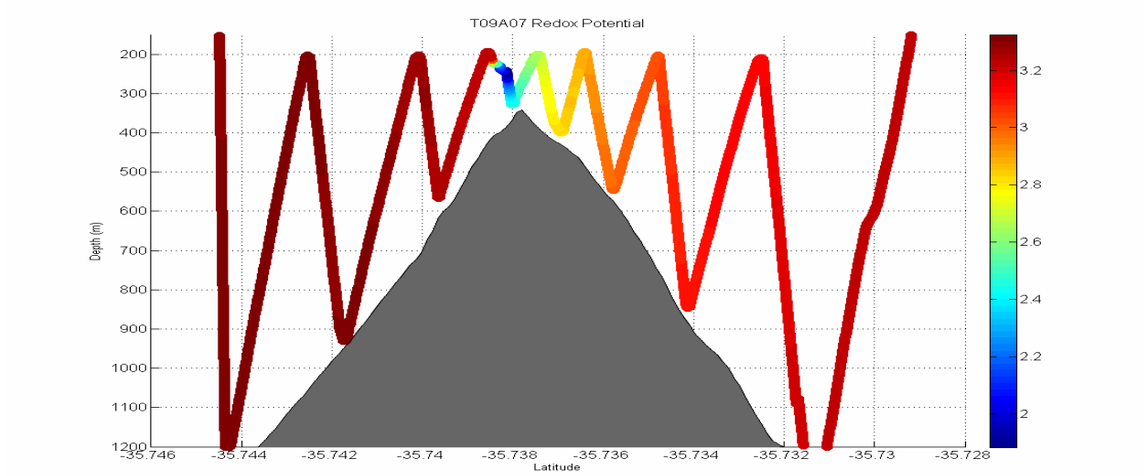

3a)

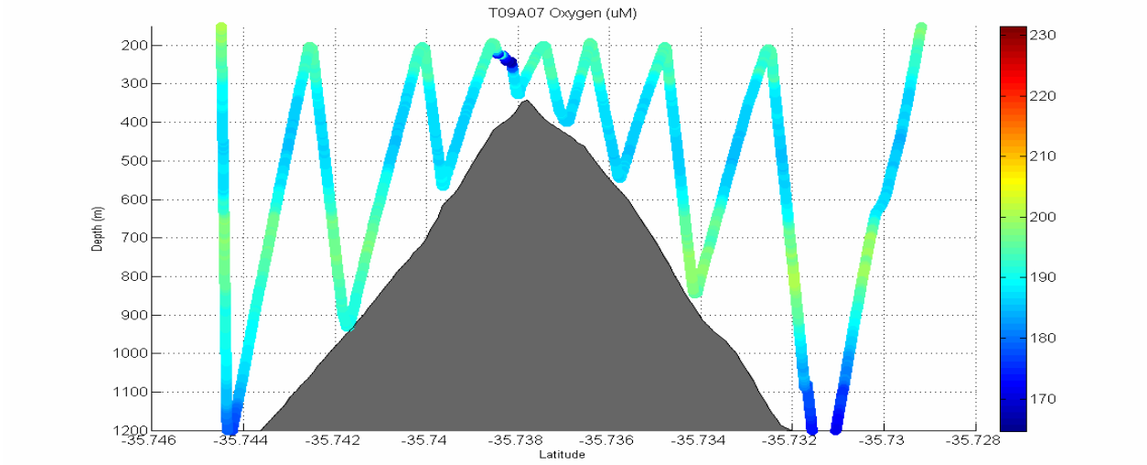

3b)

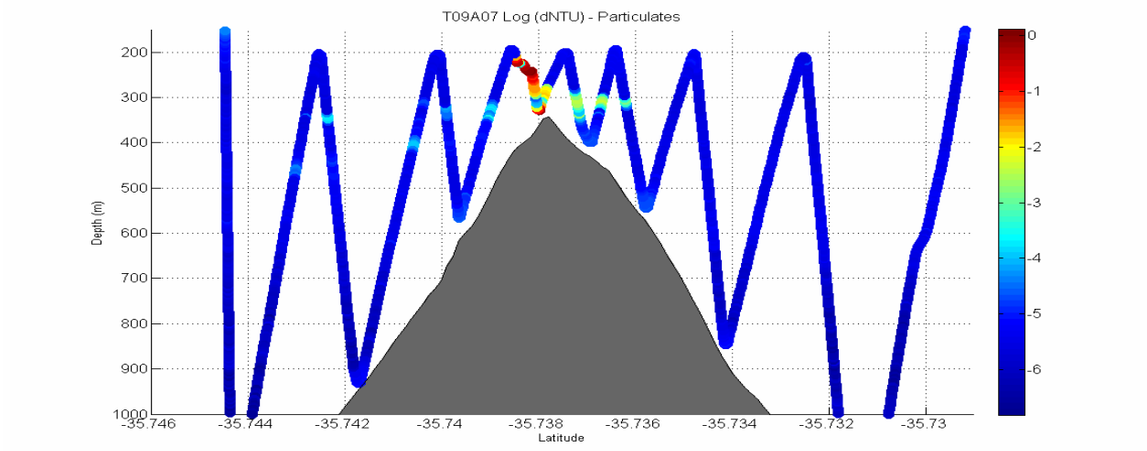

3c)

Figure 2: Tow-yo T09A05 was done from SW to NE over Rumble III and measured A) oxygen in µmol l^{-1} B) redox potential (volts) and C) log (ΔNTU) changes with depth along tow-yo T09A07 based on longitude.

In measurements from both tow-yos, the background O_2 concentration maximum of ~240 μmol l^{-1} (Figure 2b; Figure 3b) is near 100 m, with a general O_2 low to 193 μmol l^{-1} beneath the photic zone roughly 400 m depth. The O_2 increases to ~201 μmol l^{-1} near 850 m, then decreasing again with depth. The O_2 concentrations from T09A05 (Figure 2b) had a sharp contrasting low against the background at ~250 m located near 35.738° S and at 35.732° S over the summit and north over the deeper cone. This coincides with the redox potential low. The O_2 was measured as low as 174 μmol l^{-1} throughout this area, which is a difference of ~30 μmol l^{-1} from the surrounding water. T09A07 (Figure 3b) shows a similar distribution, with an oxygen low of 170 μmol l^{-1} located at 35.739° S at depths of ~240 m. This O_2 minimum is shallower in depth than the observed general background O_2 low in measured in both towyos. The O_2 anomaly (Table 1) between the expected oxygen trend with depth was calculated by curve fitting a polynomial line to T09A05 and T09A07 data, excluding the low measurements within the plume. The polynomial curve fit for T09A05 had a standard deviation of 1.023 μmol l^{-1} while T09A07 had a standard deviation of 1.16 μmol l^{-1} . The O_2 anomaly for the vertical cast T09A09 was calculated using the fitted curve from T09A05 due to the better fitting line.

The particulates concentration are presented as Log (ΔNTU) to bring out slight variability. Towyo T09A05 (Figure 2c) are near 6 Log(ΔNTU) or higher within most of the water column except for a small, high concentration of particles located at 35.738° S over the peak of the volcano and at 35.733-35.729° S north of the peak. For T09A07 (Figure 3c), one location of low Log(ΔNTU), high particulates, is near 35.738° S at ~240 m by the summit of the volcano. Closer to the summit at ~300 m, is a low level lateral particulate concentrations is located in the region between 35.738° S to 35.734° S.

Methane (Table 1) was measured adjacent to and within the hydrothermal plumes over Rumble III. The hydrothermal plumes were determined based on in situ sensor readings. For

survey T09A05, CH_4 concentrations ranged between 2.41 nmol l^{-1} to 12.32 nmol l^{-1}. For tow-yo, T09A07, methane concentrations ranged between 3.20 and 4.84 nM. Methane concentrations from vertical cast V09A09 ranged from 4.28 to 4.72 nmol l^{-1} with one high concentration of 13.01 nmol l^{-1}.

Methane variability

Methane measurement accuracy was low as CH_4 duplicates measured from the same Niskin bottles had standard deviations that ranged from as high as 84.6 % down to 5.7 % of measured concentrations. The 10 ppm standard run between samples run had a standard deviation of 1.8% and the air concentrations standard deviation of 5.6%. The difference of methane measurements in water samples can result from numerous parts of the methane measurement procedure from water being trapped in the Niskin bottle, to how the GC's signal was integrated. Other possible ways of introducing error includes efficiency of the flame detector in the GC, and small differences in atmospheric pressure and temperature over the course of measuring a collection of samples (Eric Olsen, pers com.) Ambient air concentrations were measured before and after running the water samples. A drift in air concentrations was documented for several casts, with the largest drift of 0.2 ppm while running CH_4 samples from running samples from T09A05. The drift is likely due to changes in atmospheric conditions such as temperature and pressure.

Ambient air, with an average concentration of 1.8 ppm of methane, could potentially introduce artificially higher CH_4 concentrations if introduced during the sampling or through a leaky stopcock on the syringe. This could be a source of the large error because even the smallest amount of air results a noticeable increase of CH_4 since much of the samples had concentrations as low as 2.41 nmol l^{-1} (.05 ppm). The measured CH_4 concentrations were also near the lower limit of detection in the GC, leading to the increase in error. Many of the CH_4 duplicates have a

high standard deviation while other duplicates show very minimal difference (Table 1). Because many of the possible errors sources, much of the sampling process could only have caused a limited change in individual concentrations since standards and air concentrations have small % standard deviation and the use of a headspace to strip methane from the water is estimated to be 95% effective (Lilley et al. 1996). Due to this, it is believed that contamination with ambient air is the source of the large differences. The higher concentrations are assumed to be inaccurate and duplicate standard deviations that are more than 50% of the concentrations, the higher concentration is disregarded in the analysis.

The CH_4 concentration measured over Rumble III, not including the disregarded measurements, was highest at 4.84 nmol l^{-1} at the depth of 241.4 m (Figure 4). From the vertical cast, CH_4 concentrations ranged from 4.28 to 4.62 nmol l^{-1} at three different plumes as detected by the LBSS (Figure 5).

Table 1: Measured CH4 concentrations and in situ sensor measurements over Rumble III. The symbol * designates concentrations that are more than 50% standard deviation of the concentrations between duplicates.

Cast	ΔNTU	Redox	Longitude	Latitude	Depth (m)	Oxygen (umol/l)	Oxygen anomaly	CH4 (ppm)	CH4 (nmol/l)	% Standard Deviation
T09A05	0.1068	2.837	178.4881644	-35.7302095	254.48	189.62	-7.35	0.10	4.43	-
T09A05	0.1068	2.837	178.4881644	-35.7302095	254.48	189.62	-7.35	0.26*	11.02*	65.93 %
T09A05	0.0157	3.177	178.4789102	-35.7146070	714.02	198.71	-	0.15*	6.49*	50.73 %
T09A05	0.0157	3.177	178.4789102	-35.7146070	714.02	198.71	-	0.07	3.16	-
T09A05	0.0146	3.151	178.4793338	-35.7153087	660.52	194.36	-	0.05	2.41	-
T09A05	0.0146	3.151	178.4793338	-35.7153087	660.52	194.36	-	0.14*	6.25*	66.60 %
T09A05	0.0168	2.836	178.4904142	-35.7338806	542.12	191.98	-	0.17*	7.66*	54.15 %
T09A05	0.0168	2.836	178.4904142	-35.7338806	542.12	191.98	-	0.08	3.42	-
T09A05	0.5316	2.268	178.4930806	-35.7383075	268.19	174.27	-22.57	0.26*	12.32*	84.60 %
T09A05	0.5316	2.268	178.4930806	-35.7383075	268.19	174.27	-22.57	0.07	2.9	-
T09A07	0.3140	2.430	178.49660577	-35.73833426	223.27	186.51	-12.74	0.18	4.08	-
T09A07	0.9866	1.990	178.49717937	-35.73822072	241.70	172.47	-26.67	0.17	4.05	-
T09A07	0.9866	1.990	178.49717937	-35.73822072	241.70	172.47	-26.67	0.15	3.20	-
T09A07	1.0673	1.906	178.49717937	-35.73822072	241.39	170.36	-28.75	0.18	4.66	-
T09A07	1.0673	1.906	178.49717937	-35.73822072	241.39	170.36	-28.75	0.23	4.84	-
T09A07	0.4793	2.449	178.49833600	-35.73795563	325.46	192.13	0.53	0.14	3.36	-
V09A09	0.0525	3.089	178.4934733	-35.7376200	330.05	191.95	-.15	0.57*	13.01*	63.23 %
V09A09	0.0525	3.089	178.4934733	-35.7376200	330.05	191.95	-.15	0.22	4.62	-
V09A09	0.0123	3.113	178.4934733	-35.7376200	278.45	195.73	-36	0.23	4.72	-
V09A09	0.0123	3.113	178.4934733	-35.7376200	278.45	195.73	-36	0.19	4.28	-
V09A09	0.0237	3.042	178.4934733	-35.7376200	241.61	199.73	-07	0.13	4.29	-

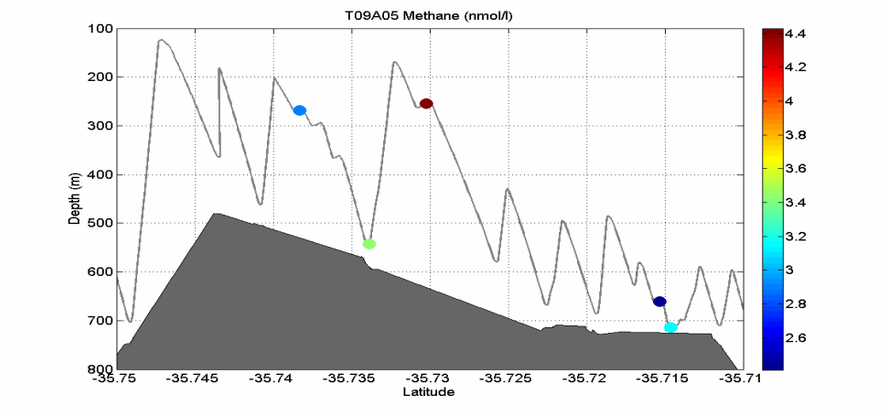

4a)

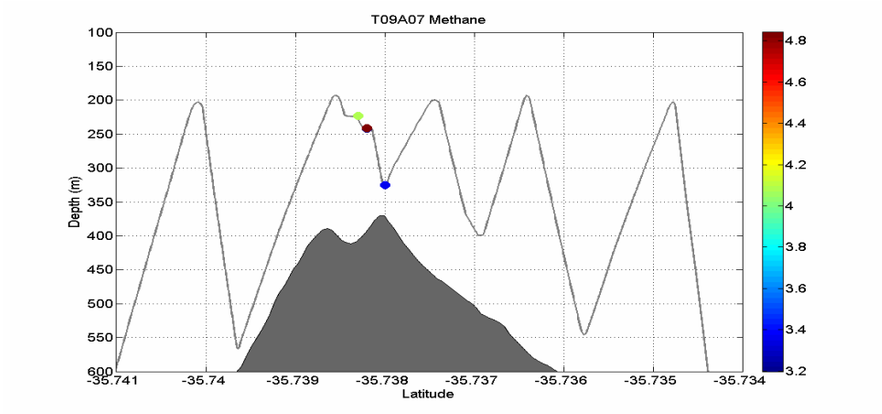

4b)

Figure 4: Niskin bottle locations and methane concentrations for a) T09A05 and b) T09A07 along with the CDTO trackline (grey line). Topography is determined based on altimeter readings on CTDO.

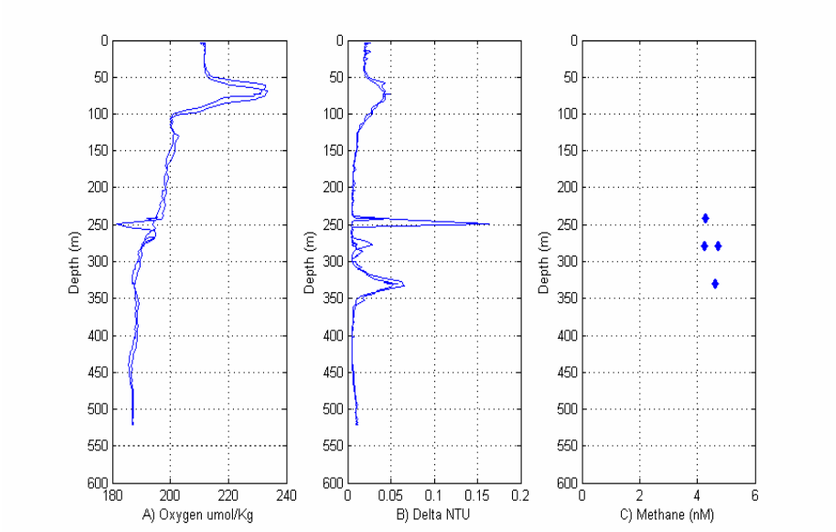

Figure 5: Distribution of Oxygen, Nephydral (ΔNTU) and Methane concentrations with depth throughout the vertical cast V09A09.

Discussion

Hydrothermal plumes, an important aspect of ocean dynamics, were detected over and around Rumble III by the higher particulates in the water column, an increase in reduced species and a reduction of oxygen (Figure 2, Figure 3). The particulates and redox show a presence of a plume between the summit and up to 200 m in both towyos and in the vertical cast. The highest concentration was detected at ~240 m in redox potential, oxygen and particulates. A higher concentration of the plume was detected in T09A07 towyo (Figure 3a). For example, the LBSS showed the highest particles of up to 0.9 ΔNTU (Table 1) in comparison to .53 ΔNTU measured during T09A05. There was also a decrease in redox potential from 2.2 volts to 1.9 between the two towyos. The O_2 had a difference of only 3 μmol l^{-1} between the lowest measurements from each of the towyos. The increase of particulates and decrease of ΔNTU can be inferred as T09A07 got closer to the hydrothermal plume source in comparison to T09A05.

The direction of the plume can be interpreted through concentration and location. The hydrothermal plume signals shows up fairly strong in several of the tow-yo depth cycle of T09A05 and only in one depth cycle of T09A07. The generally lower background redox potential measured on one side of the volcano versus the other side during the surveys (Figure 2a, Figure 3a) that is believed to be caused by a lag in the sensor after going through the plume. It is reasonable to assume that T09A05 was more in the direction of the plume while T09A07 was more perpendicular to the plume. T09A05 was performed from the northwest towards the southeast direction with the highest concentration over the summit at ~240 m depth and decreases in concentration moving north (Figure 2c). Based on these assumptions, the plume appears to be moving in the northwest direction, aligned with T09A05. Currents are the major mechanism of moving hydrothermal plumes horizontally. The current velocities during the tow-

yos were measured in the north-northwest direction at 0.15 - 0.20 m s^{-1} (A. Belcher. Pers. com.) corresponding with tow-yo data.

The estimated plume height can give a correlation of the heat being released (heat flux) and type of vent (Lupton. 1995). The hydrothermal vent depth is estimated at 350 m based on T09A07 log(ΔNTU) (Figure 3c) as it shows a high concentration near the summit of the volcano. The plume height is roughly 240 m based on both tow-yo surveys and the vertical cast. That equals to a rise height of 110 m, which is on the low side for a black smoker as a typical black smoker has an estimate rise height between 150-500 m (Lupton. 1995). This suggests the hydrothermal plumes are potentially derived from a slightly cooler white smoker that has a temperature range of 260-300° C (Tivey. 1995)

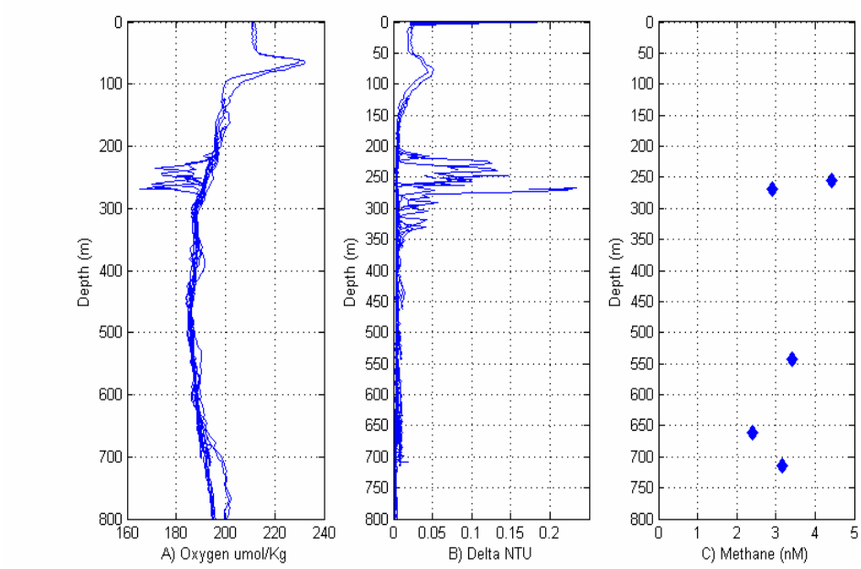

Figure 6: Vertical distribution of A) Oxygen, the B) particulate distribution and C) methane (nmol l^{-1}) during tow-yo T09A05

Methane concentrations measured over Rumble III ranging from 2.90 to 4.84 nmol l^{-1} from CTDO Niskin bottles. These concentrations have lower values for hydrothermal vents in general but are similar to the average measured CH_4 concentrations over a variety of hydrothermal vents including several locations along East Pacific Rise, segments of MAR and

Juan de Fuca south cleft (Gharib et al. 2005). The CH_4 concentrations measured on this cruise are also close to values of 1.4 - 4.0 nmol l^{-1} measured within hydrothermal plumes over the nearby Brothers volcano (de Ronde et al, 2005). CH_4 measured during T09A05 (Figure 6) was taken near the main plumes along with three bottles at deeper depths. The deeper CH_4 concentrations do not correlate with any particulates, a drastic decrease in oxygen or increase in reduced species. With this in mind, we can assume that ~3 nmol l^{-1} might be the CH_4 of the background water at that depth although the locations are over Rumble III caldera (Figure 2). Based on model estimates for open ocean CH_4 concentration, there is should be 1-2 nmol l^{-1} of methane at that depth. (Nihous and Masutani. 2006) making the measured concentration higher than predicted for open ocean.

The general background oxygen low was detected between the depths of 350-600 m (Figure 2b; Figure 3b). The typical oxygen profile has higher concentrations in the surface waters, which is produced from the photosynthesis process, then with depth, the O_2 is consumed and decreases (Najjar and Keeling. 1997) The two tow-yo profiles detected an increase in O_2 at~800m. With little data on area around the volcano, it is difficult to distinguish the cause of the increase in O_2. One possibility is winds driven mixing of O_2 to depth with a defined oxygen consumption zone where organic material is decomposing (Najjar and Keeling. 1997) that produces CH_4. The measured CH_4 within this zone was higher than a general estimated open ocean distribution which supports the theory.

The oxygen minimum, as seen in the plume above Rumble III, is a common characteristic of hydrothermal venting (Jannasch 1995). This is assumed to be caused by the presence of reduced species such as H_2S, Fe^{2+}, H_2 and CH_4 that are formed through interactions with high temperature basaltic rock. These reduced species have an affinity for O_2 as an electron acceptor, therefore reducing the O_2 concentration in the water (Jannasch and Mottl. 1985).

Chemosynthetic organisms produce energy through the use of inorganic chemical reactions. This provides the bases for the biological communities in and around hydrothermal vents (McCollom. 2000). The oxidation of reduced species within hydrothermal plumes by a variety of bacteria that are capable of oxidizing sulfur, hydrogen, nitrate, iron, manganese, methane and carbon monoxide by reacting with O_2 in oxygen rich water. In the absence of O_2, other species such as NO_3^{2-}, SO_4^{2-}, CO_2 reacts with reduced species. The reduced species primarily utilized for chemosynthesis are H_2S, H_2 and CH_4 (Jannasch and Mottl. 1985). Reduced species in hydrothermal plumes located in the deep ocean (≥1000 m) react with the oxygen forming anoxic conditions. The hydrothermal plumes situated over Rumble III are located near the ocean surface, a location of highly oxygenated waters due photosynthetic production in the photic layer and surface-atmosphere interactions. Reacting with O_2 is energetically favored over other species so species such as NO_3^{2-}, SO_4^{2-}, or CO_2 (McCollom. 2000) which could possibly be in higher concentrations at this location than at hydrothermal vent locations in the deep ocean. Although interactions involving the photosynthesis process found in the surface waters would make this comparisons difficult.

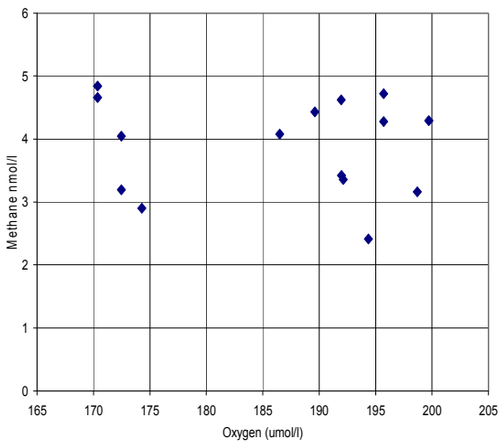

7a)

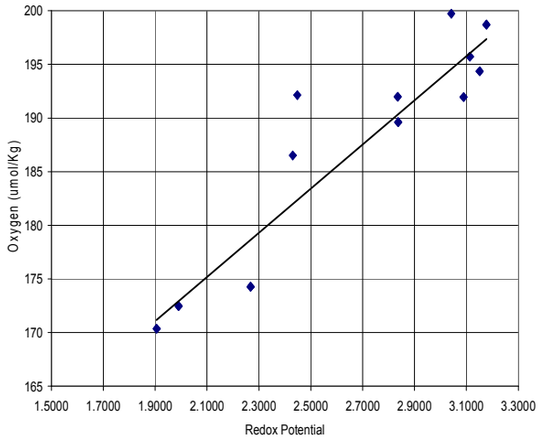

7b)

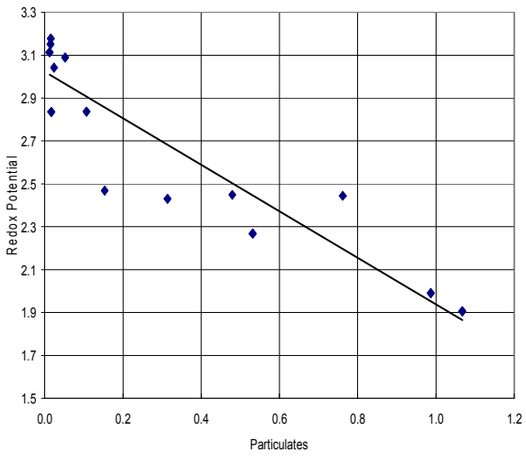

7c)

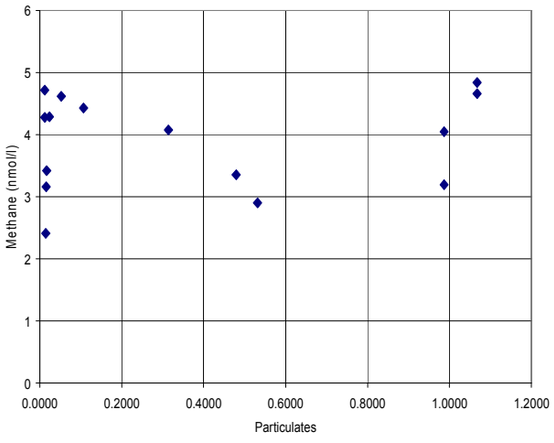

7d)

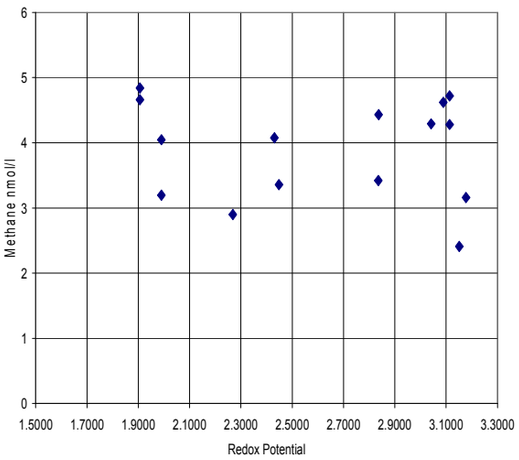

7e)

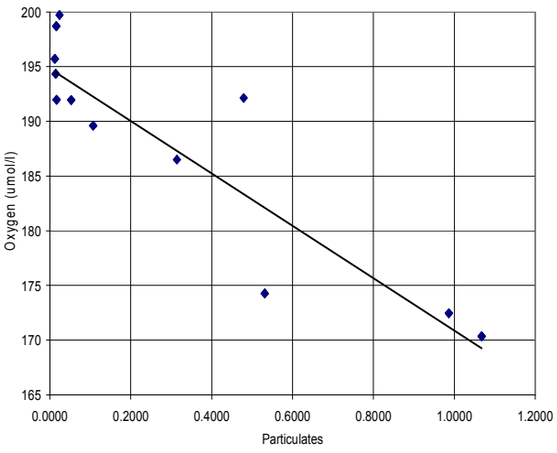

7f)

Figure 7: CTDO bottle data collected during T09A05, T09A07 and V09A09 of Methane, redox potential and oxygen.

Microbial oxidation is the method of degradation of CH_4 that is present in aerobic conditions by methanotrophic bacteria through the reaction (Jannasch and Mottl. 1985):

$$2CH_4 + 2O_2 = 2[CH_2O] + 2H_2O \quad (1)$$

Unfortunately, measurements taken over Rumble III do not show a definite correlation between oxygen and methane (Figure 7a). Also the CH_4 concentrations taken during the vertical cast, V09A09 (Figure 5), show not much difference between the CH_4 while there is a small variation in oxygen concentration with depth. Other chemical reactions that could be interacting with the O_2 are H_2 and sulfur, which is more spontaneous and therefore are used up at a faster rate, although as they disappear, the methane becomes a more viable source (McCollum. 2000). The low correlation between redox potential and CH_4 (Figure 7e) is evidence of other reduced species within the plumes and that the redox potential is associated with the particulates of the hydrothermal plumes (Figure 7c).

A way to determine if the oxygen is caused by other reduced species is by comparing the redox potential to the O_2 concentration (Figure 7b). The relationship between the redox potential and oxygen, at a glance, appears to be a linear correlation. This is most likely due to the oxidation of chemical species either biogenetically or spontaneous which are present within the hydrothermal plume based on that lower O_2 concentrations are correlated with increased particulates (Figure 7f). These other species capable of oxidize O_2 include sulfur, hydrogen, iron, manganese, and carbon monoxide (Jannasch. 1995) The oxidation of precipitated elemental sulfur, in particular, is the largest single source of energy based on chemically derived energy (McCollum. 2000).

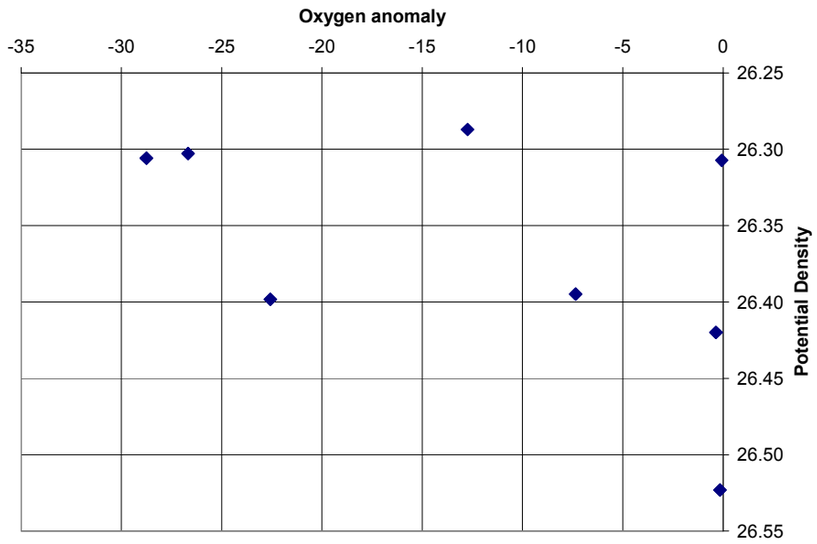

Figure 8: The oxygen anomaly between depths of 170-330 m.

The hydrothermal plumes are located near to the photic zone and therefore some of the CH_4 could be derived from organic decomposition that is estimated to increase the background CH_4 concentration to ~3 nmol l^{-1} at ~150 m depth for open ocean (Nihous and Masutani. 2006). The CH_4, in comparison to particulate concentration (Figure 7d) does decrease with decreasing particulates, then increase again towards 0.0 ΔNTU. The high variability of CH_4 near to 0.0 ΔNTU is may be due to measuring the CH_4 at several depths near and far from the photic zone. The CH_4 decrease at high particulates may be due to the rapid oxidation of CH_4 within the hydrothermal plume (Cowen, 2002). The CH_4 concentrations of ~4.6 nmol l^{-1} at 1.1 ΔNTU could be hydrothermally based.

The combination of low oxygen, high particulate and high redox potential anomaly in the water column is only seen within the plume detected in and around 250 m depth. A characteristic of hydrothermal plume is rises to a density horizon and spread out laterally (Lupton. 1995). Comparing the calculated oxygen anomaly with density (Figure 8), there are two different potential densities apparent at ~26.30 and ~26.40, which is possibly plumes from two difference sources. The potential density of 26.30 correlates to the depths of 228-241 m while the potential

density of 26.40 correlates to 254-268 m in depth. Lack of oxygen anomaly data over Rumble III makes its difficult to identify oxygen anomaly trends. The vertical cast over the summit of Rumble III, detected particulates (Figure 5) at ~245m, 275m and 330m evident of three plumes.

Conclusion

Methane concentrations in and around hydrothermal vents over Rumble III was found to contain a large error in duplicate run from the same Niskin bottles. This was assumed to be primarily from contamination from ambient air that has a concentration of ~1.8 ppm. The ambient air concentrations are a significant amount considering the CH_4 water samples were measured as low as 0.05 ppm. To compensate for the significant error, the higher measurement that has a standard deviation larger than 50% of the concentration, were eliminated.

Based on the measured sensors, the main hydrothermal plumes were detected near 250 m, while traces of hydrothermal plumes were detected at ~275 m and 330 m over Rumble III. The plumes was characterized by low oxygen, high particulate and low redox potential, an indicator of high reduced chemical species. Measurements from sensor readings were the highest for particulates and lowest for redox potential during the T09A07 tow-yo at depths around 250 m. The very low correlation of CH_4 with particulates and oxygen is evidence that other processes interacting with the CH_4 concentrations such as exchanges with surface waters and photosynthetic based biology.

Based on the distribution of hydrothermal plume material, the plume was carried in the northwest direction. At that time, the water current direction over Rumble III at the time of measurement was in the same direction. It is estimated that the vents are mid temperature white smokers due to the calculated rise high from tow-yo in situ measurements. Although the calculated rise height is only 40 m off from the ‘typical’ black smoker rise height.

As to further expand this study, the addition of δC^{13} of CH_4 and manganese concentrations would be beneficial. As this is a high biologically active area and therefore it is difficult to determine if the measured CH_4 is biogenetically or abiogenetically produced. The δC^{13} of the CH_4 will be able to determine the source since biologically produced CH_4 has an isotopically lighter δC^{13}. The manganese will help gain a better idea of interactions within the hydrothermal system as the CH_4 to manganese ratio will change as the system changes.

References

Baker, E.T, D. A. Tennant, R.A. Feely, G.T. Lebon, and S.L. Walker. 2001. Field and laboratory studies on the effect of particule size and composition on optical backscattering measurements in hydrothermal plumes. Deep-Sea Research I. **48**:593-604

Cowen, J.P., X. Wen, and B.N. Popp. 2002. Methane in aging hydrothermal plumes. Geochimica et cosmochimica Acta, **66**: 3563-3571

De Angelis, M.A., M.D. Lilley, E.J. Olson, and J.A. Baross. 1993. Methane oxidation in deep-sea hydrothermal plumes of the Endeavour Segment of the Juan de Fuca Ridge. Deep-sea Research I. **40**: 1169-1186.

De Ronde, C. E. J., M. D. Hannington, P. Stoffers, I. C. Wright, R. G. Ditchburn, A. G. Reyes, E. T. Baker, G. J. Massonth, J. E. Lupton, S. L. Walker, R. R. Greene, C. W. R. Soong, J. Ishibashi, G. T. Lebon, C. J. Bray, and J. A. Resing. 2005 Evolution of a Submarine Magmatic-Hydrothermal System: Brothers Volcano, Southern Kermadec Arc, New Zealand. **100**: 1097–1133.

De Ronde, C. E.J., E.T. Baker, G.J. Massoth, J.E. Lupton, I.C. Wright. R.A. Feely, and R.R. Greene. 2001. Intra-oceanic subduction-related hydrothermal venting, Kermadec arc, New Zealand. Earth and Planetary Science Letters. **193**: 359-369.

Gharib, J.J, F.J. Sansone, J.A. Resing, E.T. Baker, J.E. Luption, and G.J. Massoth. 2005. Methane dynamics in hydrothermal plumes over a superfast spreading center: East Pacific Rise, 27.5 -32.3 S. Journal of Geophysical Research. **110**. B10101. doi:1029/2004JB003531.

Jannasch, H. W. and M. J. Mottl. 1985. Geomicrobiology of Deep-Sea hydrtothermal Vents. Science, New Series. 229(4715): 717-725

Jannasch. 1995. Microbial interactions with hydrothermal fluids. 273-296. In: Hydrothermal systems: Physical, Chemical, Biological and Geological Interactions. Geophysical Monograph 91

Kadko, D. J. Baross, and J. Alt. 1995. The Magnitude of global implications of hydrothermal flux. 446-466 In: Hydrothermal systems: Physical, Chemical, Biological and Geological Interactions. Geophysical Monograph 91

Lilley, M.D., D.A. Butterfield, E.J. Olson. J.E. Lupton. S.A. Macko, and R.E. McDuff. 1993. Anomalous CH4 and NH4+ concentrations at an unsedimented mid-ocean-ridge hydrothermal system. Nature. **364**: 45-47

Lilley, M.D., M.A. de Angelis, and E.J. Olson. 1996. Methane concentrations and estimated fluxes. Miyy. Internat. Verein. Limnol. **25**: 187-196.

Lupton, J.E. 1995. Hydrothermal Plumes: Near and Far Field. 317-346. In: Hydrothermal systems: Physical, Chemical, Biological and Geological Interactions. Geophysical Monograph 91

McCollom T.M. 2000. Geochemical constraints on primary productivity in submarine hydrothermal vent plumes. Deep Sea Research I. **47**:85-101.

Mottl, M.J., F.J. Sansone, C.G. Wheat, J.A. Rising, E.T. Baker, and J.E. Lupton. 1995. Manganese and methane in hydrothermal plumes along the East Pacific Rise, 8 40’ to 11 50’ N. Geochimica et cosmochimica Acta. **99**: 4147-4165.

Najjar, R.G. and R.F. Keeling. 1997. Analysis of the mean annual cycle of the dissolved oxygen anomaly in the world ocean. Journal of Marine Research. **55**:117-151

Nihous, G.C. and S.M. Masutani. 2006. A Model of methane concentration profile in the open ocean. Journal of Marine Research. **64**: 629-650.

Prol-Ledesma, R.M., P.R. Dando, C.E.J. de Ronde. 2005. Preface: Special issue on “shallow-water hydrothermal venting”. Chemical Geology. **224**:1-4

Tivey, M.K. 1995. Modeling chimney growth and association fluid flow at seafloor hydrothermal vent sites. 158-177. In: Hydrothermal systems: Physical, Chemical, Biological and Geological Interactions. Geophysical Monograph 91

Von Damm, K.L. 1995.Controls on the Chemistry and temporal variability of seafloor hydrothermal fluids. 222-247. In: Hydrothermal systems: Physical, Chemical, Biological and Geological Interactions. Geophysical Monograph 91

Welhan, J.A. 1988. Origins of methane in hydrothermal systems. Chemical Geology. **71**: 183-198.

Wright, I.C. 1994. Nature and tectonic settings of the southern Kermadec submarine arc volcanoes: An overview. Marine Geology. **118**: 217-236.

Wright, I.C., P Stoffers. . Hanington, C.E.J. de Ronde, P. Herzig, I.E.M. Smith, and P.R.L. Browne. 2002. Towed-camera investigations of shallow-intermediate water-depth submarine stratovolcanoes of the southern Kermade arc, New Zealand. Marine Geology. **185**: 207-218

Wright, I.C., T.K. Worthington, and J.A. Gamble. 2006. New multibeam mapping and geochemistry of the 30-35 S sector, and overview, of southern Kermadec arc volcanism. Journal of Volcanology and Geothermal Research. **149**: 263-296

Carlson, J. 2007. Development of an optimized dissolved oxygen sensor for oceanographic profiling. Sea-Bird Electronics.